

# Vacuum-UV-excited Photoluminescence and Scintillation Properties of CsCl Transparent Ceramics and Single Crystal

Hiroimi Kimura,<sup>1\*</sup> Takumi Kato,<sup>1</sup> Daisuke Nakauchi,<sup>1</sup>  
Masanori Koshimizu,<sup>2</sup> Noriaki Kawaguchi,<sup>1</sup> and Takayuki Yanagida<sup>1</sup>

<sup>1</sup>Division of Materials Science, Nara Institute of Science and Technology (NAIST),  
8916-5 Takayama-Cho, Ikoma, Nara 630-0192, Japan

<sup>2</sup>Department of Applied Chemistry, Graduate School of Engineering, Tohoku University,  
6-6-07 Aoba, Aramaki, Aoba-ku, Sendai, Miyagi 980-8579, Japan

(Received November 26, 2018; accepted March 25, 2019)

**Keywords:** transparent ceramic, CsCl, VUV, scintillation, thermally stimulated luminescence

CsCl transparent ceramics were prepared by the spark plasma sintering (SPS) method, and their optical, scintillation, and dosimetric properties were investigated. To evaluate the potential of the transparent ceramics, a CsCl single crystal was prepared by the vertical Bridgman–Stockbarger method. Regarding the luminescence properties, the vacuum UV (VUV)-excited photoluminescence (PL) and scintillation spectral features of the transparent ceramics were similar to those of the single crystal. Concerning the thermally stimulated luminescence (TSL) properties, the minimum detection limit of the transparent ceramics was 0.01 mGy.

## 1. Introduction

Ionizing radiation detectors often utilize phosphor materials, and such detectors are mainly classified into two types: scintillation detectors and dosimeters. The former type uses scintillators, which convert absorbed energy of ionizing radiation immediately into visible photons, and then the photons are detected by a photodetector [e.g., photomultiplier tube (PMT) and photodiode]. They have been widely used in various fields, such as medicine<sup>(1)</sup> and security,<sup>(2)</sup> and particularly in the presence of hidden special nuclear materials (in the case of SNM environmental monitoring<sup>(3)</sup> and high-energy physics).<sup>(4)</sup> To improve the performance of scintillation detectors, scintillators require high effective atomic number, high light yield, short decay time, and low afterglow. In contrast, the latter type uses storage phosphors, which store the energy of ionizing radiation in the form of trapped electrons and holes at localized trapping centers. The trapped charges can be released by heat (thermally stimulated luminescence: TSL) or light (optically stimulated luminescence: OSL) to emit photons. The TSL or OSL intensities are proportional to the radiation dose and have been used in individual radiation monitoring<sup>(5–7)</sup> and imaging plates (IPs)<sup>(8,9)</sup> as dosimetry applications. Although these two fields, that is, scintillators and ionizing-radiation-induced storage phosphors, developed independently, the complementary relationship between these two phenomena has been pointed out, and it is

\*Corresponding author: e-mail: kimura.hiroimi.kf1@ms.naist.jp  
<https://doi.org/10.18494/SAM.2019.2186>

important to evaluate both properties in each material to gain a deeper understanding of the ionizing-radiation-induced luminescent phenomena.<sup>(10–12)</sup>

Thus far, most scintillators have been used mainly in the form of bulk single crystals because of the high transparency<sup>(13–16)</sup> and density, although single crystals have some disadvantages for mass production (e.g., high cost and low mechanical strength). In recent years, transparent ceramics have emerged as an alternative to single crystals along with the progress of synthesis technologies.<sup>(17–19)</sup> The advantages of transparent ceramics are high mechanical strength and low cost in comparison with those of single crystals. Moreover, it has been reported that some transparent ceramics such as GAGG:Ce<sup>(20)</sup> and LuAG:Ce<sup>(21)</sup> show higher scintillation light yields than single crystal counterparts. Thus, transparent ceramics have a high potential as radiation detectors.

CsCl can be applied in ionizing radiation detectors and IPs as scintillators and storage phosphors because it has a high effective atomic number ( $Z_{eff} = 51.9$ ) comparable to those of conventional scintillators such as CsI ( $Z_{eff} = 54.1$ ) and NaI ( $Z_{eff} = 50.8$ ). Moreover, it is known that CsCl shows Auger-free luminescence (AFL), the decay time of which is very short (a few nanoseconds).<sup>(22,23)</sup> Up to now, photoluminescence (PL),<sup>(24)</sup> scintillation,<sup>(25)</sup> and TSL properties<sup>(26)</sup> of CsCl have been reported in the literature. However, almost all the studies were performed on the bulk single crystals, and there has been no report on transparent ceramics. In this study, CsCl transparent ceramics were formed by the spark plasma sintering (SPS) method, and their optical, scintillation, and dosimetric properties were studied. To evaluate the potential of the transparent ceramics, a CsCl single crystal was also investigated for comparison.

## 2. Experiment

CsCl transparent ceramics were synthesized by the SPS method using Sinter Land LabX-100 in vacuum. High-purity CsCl (>99.999%, Mitsuwa Chemical) was loaded to a cylindrical graphite die and held between two graphite punches. SPS was performed by applying a high-current DC pulse while applying uniaxial pressure along the axis of graphite punches. During the sintering, the temperature was increased from 20 to 500 °C at a rate of 48 °C/min and then held for 10 min while applying a pressure of 6 MPa. After the synthesis, the synthesized sample was polished by sandpaper (3000 grit). On the other hand, a CsCl single crystal was grown by the vertical Bridgman-Stockbarger method, which is conventionally used for preparing halide scintillators.<sup>(27–29)</sup> The raw powder of CsCl was loaded into a quartz ampule and dried in two steps, namely, heating at ~150 °C for 1 h and that of ~400 °C for 2 h in vacuum. Next, the dried powder was enclosed in a vacuum-sealed quartz ampule, and the sealed ampule was set in a Bridgman furnace (VFK-1800, Crystal Systems Corp.). During the crystal growth, the temperature was 695 °C and the pulling-down rate was 10 mm/h. The obtained single crystal rod was cut and mechanically polished with sandpaper (3000 grit). The size of the single crystal is the same as that of the transparent ceramics after the polishing process, and the processed samples were used for the following measurements.

As optical properties, diffuse transmittance spectra were measured using a spectrophotometer (SolidSpec-3700, Shimadzu) across the spectral range from 200 to 850 nm

with 1 nm intervals. The PL quantum yields (QYs) were obtained using a Quantaaurus-QY spectrometer (C11347, Hamamatsu Photonics). The PL spectra and decay curves were evaluated using a Quantaaurus- $\tau$  spectrometer (C11367, Hamamatsu Photonics). Moreover, the excitation spectra were measured at room temperature under synchrotron irradiation at the UVSOR synchrotron facility (BL-7B). The measurement spectral range for excitation in the vacuum UV (VUV) region was from 50 to 200 nm.

To investigate scintillation properties, X-ray-induced scintillation spectra were measured using our original setup.<sup>(20)</sup> An X-ray generator (XRB80P&N200X4550, Spellman) equipped with a conventional X-ray tube was used. The X-ray tube had a W anode target and was operated with the tube voltage and current of 40 kV and 1.2 mA, respectively. X-ray-induced scintillation decay curves were evaluated using an afterglow characterization system.<sup>(30)</sup>

As dosimetric properties, TSL glow curves were measured using a TSL reader (TL-2000, Nanogray Inc.) after irradiation with X-rays (10 mGy).<sup>(31)</sup> During the measurement, the temperature range was from 50 to 350 °C, and the heating rate was 1 °C/s. To obtain dose response functions, a series of TSL glow curves were measured by varying the irradiation dose from 0.01 to 1000 mGy.

### 3. Results and Discussion

#### 3.1 Sample

Figure 1 shows photographs of the CsCl single crystal and transparent ceramics. The thickness of both samples is fixed to  $\sim 0.5$  mm, and the prepared samples are visually transparent. Diffuse transmittance spectra are shown in Fig. 2. The transmittances of the crystal and ceramics in the near-UV and visible regions are  $\sim 80$  and  $\sim 70\%$ , respectively. After X-ray irradiation ( $\sim 10$  Gy), we noted that an absorption band at around 600 nm appears; it is typical for alkali halide.<sup>(32)</sup> The origin is F-centers formed by Cl vacancies.<sup>(33)</sup> The other X-ray-induced properties will be described later.

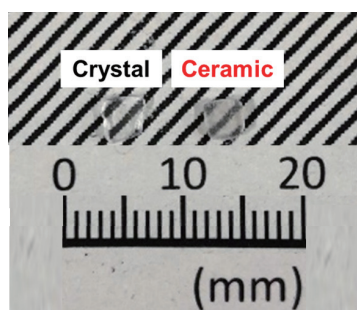


Fig. 1. (Color online) Synthesized CsCl single-crystal and transparent ceramics under room light.

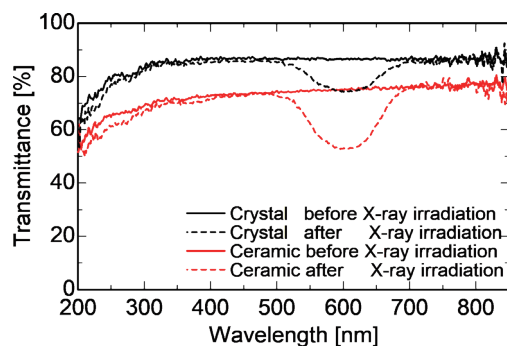


Fig. 2. (Color online) Diffuse transmittance spectra of CsCl single crystal and transparent ceramics before and after X-ray irradiation ( $\sim 10$  Gy).

### 3.2 PL properties

The PL excitation and emission spectra of the CsCl single crystal and transparent ceramics are illustrated in Fig. 3. The PL spectral features of the transparent ceramics are similar to those of the single crystal. The excitation spectra show two bands peaking at around 240 and 270 nm, and the intense and weak emission bands at around 340 and 400 nm are observed upon 270 nm excitation. According to the previous study,<sup>(24)</sup> a pure CsCl single crystal exhibits a broad band between 300 and 500 nm with the peak top of 335 nm under excitation with two bands peaking at 214 and 269 nm. The origins of the emission peaks at around 340 and 400 nm are some impurity defects.<sup>(34,35)</sup> The PL QYs of the crystal and ceramic samples are 7.6 and 2.4%, respectively.

Figure 4 shows the PL decay profiles of the single crystal and transparent ceramics monitored at 340 nm under 280 nm excitation. The decay curves of both samples were well approximated by the sum of two exponential decay functions. The faster and slower decay time constants of the two samples are  $\sim 2$  and  $\sim 88$  ns, respectively, and the faster decay time constant is consistent with the past report.<sup>(36)</sup> However, the origin of the slow component is unclear. As a possible interpretation, the origin of the slower component may be some impurity defects because the emission at around 400 nm seems broad.

The VUV-excited PL excitation and emission spectra of the CsCl single crystal and transparent ceramics are presented in Fig. 5. The spectral feature of the transparent ceramics is the same as that of the single crystal. The spectral features of excitation bands at around 140 and 190 nm and an emission band at around 400 nm corresponded to the results of the previous work,<sup>(34,37)</sup> and the origin was concluded to be some impurity defects. Figure 6 represents the VUV-excited PL decay profiles of CsCl single-crystal and transparent ceramics, where the excitation and monitoring wavelengths were 180 and 400 nm, respectively. The decay curves of both samples are approximated by a single exponential decay function. The decay time constants of the ceramic and crystal samples are 1.68 and 1.87 ns, respectively, and the origin is thought to be some impurity defects.

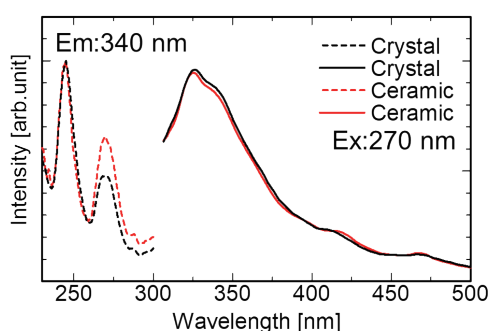


Fig. 3. (Color online) PL excitation and emission spectra of CsCl single crystal and transparent ceramics.

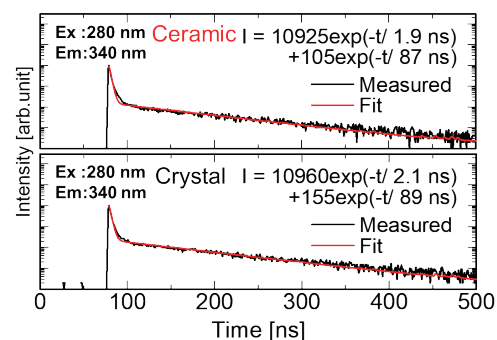


Fig. 4. (Color online) PL decay profiles of CsCl transparent ceramic (top) and single crystal (bottom). The monitoring wavelength was 340 nm, while the excitation wavelength was 280 nm.

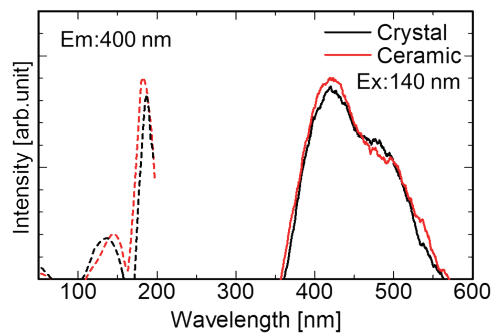


Fig. 5. (Color online) VUV-excited PL excitation and emission spectra of CsCl single-crystal and transparent ceramic samples.

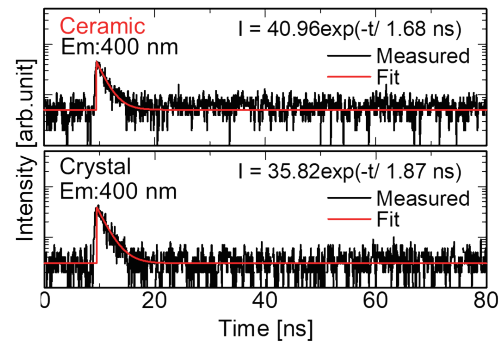


Fig. 6. (Color online) VUV-excited PL decay profiles of CsCl transparent ceramic (top) and single-crystal (bottom) samples. The excitation and monitoring wavelengths were 180 and 400 nm, respectively.

### 3.3 Scintillation properties

X-ray-induced scintillation spectra of the CsCl single crystal and transparent ceramics are presented in Fig. 7. The spectrum consists of four bands peaking at around 245, 275, 330, and 400 nm. The emission peaks at around 245 and 275 nm are typically attributed to the AFL.<sup>(23)</sup> The other emission peaks at around 330 and 400 nm have the same origin as those discussed for PL and VUV-excited PL, and these emission peaks are attributed to some impurity defects.<sup>(34)</sup> These scintillation spectral shapes are consistent with the previous research,<sup>(37)</sup> and the emission wavelength is favorable for a typical PMT. Figure 8 represents X-ray-induced scintillation decay profiles of the CsCl single crystal and transparent ceramics. Scintillation decay curves of both samples are well approximated by a single exponential decay function. The decay time constants of the ceramic and crystal samples are 1.63 and 1.51 ns, respectively, and the decay components are attributed to the mixture of the AFL and some impurity defects.

### 3.4 Dosimetric properties

Figure 9 shows TSL glow curves of the CsCl single crystal and transparent ceramics measured after X-ray irradiation ( $\sim 10$  mGy). Both samples show three glow peaks at around 75, 100, and 160 °C. The peak positions of the glow curves are consistent with the previous reports.<sup>(38,39)</sup> In addition, there are TSL signals at around 50 °C, which implies some glow peaks at temperatures below 50 °C. In the past work, several TSL glow peaks were detected at room temperature or lower.<sup>(26)</sup> The TSL dose response functions of the CsCl single crystal and transparent ceramics are shown in Fig. 10. The TSL intensity represents the integrated signals between 50 and 250 °C of the measured glow curves. The ceramics show good linearity from 0.01 to 1000 mGy with the detection limit of the crystal being 0.1 mGy. Thus, we confirmed that the ceramics show a better dosimetric property than the crystal. From the viewpoint of detector properties, the sensitivities of both samples are comparable to those of commercial dosimeters.

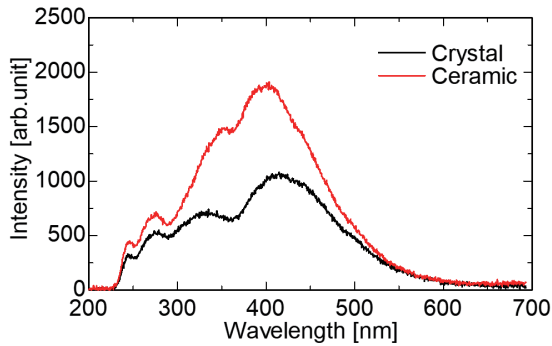


Fig. 7. (Color online) X-ray-induced scintillation spectra of CsCl single crystal and transparent ceramics.

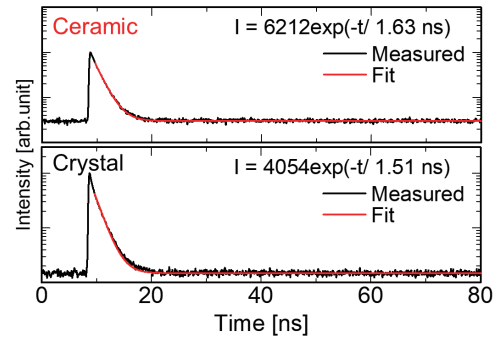


Fig. 8. (Color online) X-ray-induced scintillation decay profiles of CsCl single crystal and transparent ceramics.

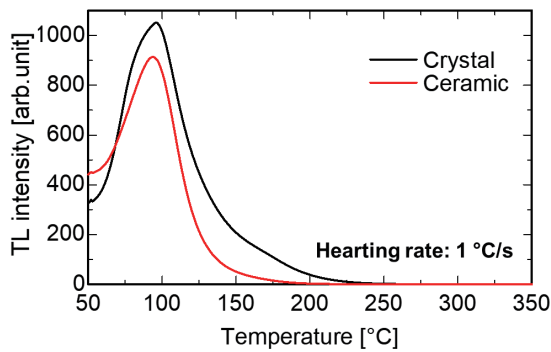


Fig. 9. (Color online) TSL glow curves of CsCl single crystal and transparent ceramics measured after 10 mGy X-ray irradiation.

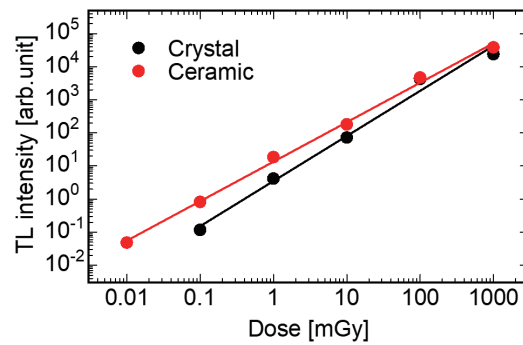


Fig. 10. (Color online) TSL dose response curves of CsCl single crystal and transparent ceramics from 0.01 to 1000 mGy.

#### 4. Conclusions

CsCl transparent ceramics were formed by the SPS method and their optical, VUV-excited PL, scintillation, and dosimetric properties were compared with those of a CsCl single crystal. Regarding the optical properties, the diffuse transmittances of the crystal and ceramics in the near-UV and visible regions were  $\sim 80$  and  $\sim 70\%$ , respectively. Compared with the single crystal, the synthesized transparent ceramic sample showed similar VUV-excited PL and scintillation spectral features. We confirmed that both samples show AFL with a very fast decay time. As the dosimetric properties, the samples were very sensitive to the X-ray dose, and the detection limit of the transparent ceramics was 0.01 mGy.

#### References

- 1 C. W. E. van Eijk: Nucl. Instrum. Methods Phys. Res., A **509** (2003) 17.
- 2 J. M. Hall, S. Asztalos, P. Bilotft, J. Church, M. A. Descalle, T. Luu, D. Manatt, G. Mauger, E. Norman, D. Petersen, J. Pruet, S. Prussin, and D. Slaughter: Nucl. Instrum. Methods Phys. Res., B **261** (2007) 337.

- 3 K. Watanabe, T. Yanagida, and K. Fukuda: *Sens. Mater.* **27** (2015) 269.
- 4 T. Itoh, M. Kokubun, T. Takashima, T. Honda, K. Makishima, T. Tanaka, T. Yanagida, S. Hirakuri, R. Miyawaki, H. Takahashi, K. Nakazawa, and T. Takahashi: *IEEE Trans. Nucl. Sci.* **53** (2006) 2983.
- 5 R. W. Christy, N. M. Johnson, and R. R. Wilbarg: *J. Appl. Phys.* **38** (1967) 2099.
- 6 Y. Hirata, K. Watanabe, S. Yoshihashi, A. Uritani, Y. Koba, N. Matsufuji, T. Yanagida, T. Toshito, and K. Fukuda: *Sens. Mater.* **29** (2017) 1455.
- 7 G. Okada, T. Kato, D. Nakauchi, K. Fukuda, and T. Yanagida: *Sens. Mater.* **28** (2016) 897.
- 8 H. Nanto, A. Nishimura, M. Kuroda, Y. Takei, Y. Nakano, T. Shoji, T. Yanagita, and S. Kasai: *Nucl. Instrum. Methods Phys. Res., A* **580** (2007) 278.
- 9 N. M. Winch, A. Edgar, and C. M. Bartle: *Nucl. Instrum. Methods Phys. Res., A* **763** (2014) 394.
- 10 T. Yanagida, G. Okada, and N. Kawaguchi: *J. Lumin.* **207** (2019) 14.
- 11 T. Yanagida: *J. Lumin.* **169** (2016) 544.
- 12 T. Yanagida: *Proc. Jpn. Acad. Ser. B* **94** (2018) 75.
- 13 I. Holl, E. Lorenz, and G. Mageras: *IEEE Trans. Nucl. Sci.* **35** (1988) 105.
- 14 P. Schotanus and R. Kamermans: *IEEE Trans. Nucl. Sci.* **37** (1990) 177.
- 15 E. Sakai: *IEEE Trans. Nucl. Sci.* **34** (1987) 418.
- 16 T. Yanagida, M. Koshimizu, G. Okada, T. Kojima, J. Osada, and N. Kawaguchi: *Opt. Mater.* **61** (2016) 119.
- 17 H. Kimura, K. Shinozaki, G. Okada, N. Kawaguchi, and T. Yanagida: *J. Non-Cryst. Solids* **72** (2018) 8916.
- 18 H. Kimura, F. Nakamura, T. Kato, D. Nakauchi, G. Okada, N. Kawaguchi, and T. Yanagida: *J. Mater. Sci. Mater. Electron.* **29** (2018) 8498.
- 19 H. Kimura, F. Nakamura, T. Kato, D. Nakauchi, N. Kawano, G. Okada, N. Kawaguchi, and T. Yanagida: *Optik* **157** (2018) 421.
- 20 T. Yanagida, K. Kamada, Y. Fujimoto, H. Yagi, and T. Yanagitani: *Opt. Mater.* **35** (2013) 2480.
- 21 T. Yanagida, Y. Fujimoto, Y. Yokota, K. Kamada, S. Yanagida, A. Yoshikawa, H. Yagi, and T. Yanagitani: *Radiat. Meas.* **46** (2011) 1503.
- 22 M. Itoh and M. Kamada: *J. Phys. Soc. Jpn.* **70** (2001) 3446.
- 23 A. Voloshinovskii: *Radiat. Meas.* **33** (2001) 565.
- 24 J. Kim, S. Ra, W. Kim, H. J. Kim, H. Park, S. H. Lee, H. Kang, S. Kim, D. Kim, and S. Doh: *J. Korean Phys. Soc.* **50** (2007) 1514.
- 25 A. Lushchik, M. Kirm, C. Lushchik, and E. Vasil'chenko: *Nucl. Instrum. Methods Phys. Res., B* **166–167** (2000) 529.
- 26 A. Lushchik, K. Ibragimov, I. Kudrjavitseva, and L. Pung: *Radiat. Eff. Defects Solids* **136** (1995) 253.
- 27 Y. Fujimoto, K. Saeki, D. Nakauchi, T. Yanagida, M. Koshimizu, and K. Asai: *Sens. Mater.* **29** (2017) 1425.
- 28 T. Sakai, M. Koshimizu, Y. Fujimoto, D. Nakauchi, T. Yanagida, and K. Asai: *Sens. Mater.* **30** (2018) 1565.
- 29 Y. Fujimoto, K. Saeki, D. Nakauchi, T. Yanagida, M. Koshimizu, and K. Asai: *Sens. Mater.* **30** (2018) 1577.
- 30 T. Yanagida, Y. Fujimoto, T. Ito, K. Uchiyama, and K. Mori: *Appl. Phys. Express* **7** (2014) 62401.
- 31 T. Yanagida, Y. Fujimoto, N. Kawaguchi, and S. Yanagida: *J. Ceram. Soc. Jpn.* **121** (2013) 988.
- 32 H. Kimura, F. Nakamura, T. Kato, D. Nakauchi, N. Kawano, G. Okada, N. Kawaguchi, and T. Yanagida: *J. Ceram. Soc. Jpn.* **126** (2018) 184.
- 33 H. Rabin and J. H. Schulman: *Phys. Rev.* **125** (1962) 1584.
- 34 A. Lushchik, E. Feldbach, A. Frorip, K. Ibragimov, I. Kuusmann, and C. Lushchik: *J. Phys. Condens. Matter* **6** (1994) 2357.
- 35 M. Itoh, K. Tanimura, and N. Itoh: *J. Phys. Soc. Jpn.* **62** (1993) 2904.
- 36 M. Itoh, Y. Bokumoto, and H. Yoshida: *J. Phys. Soc. Jpn.* **68** (1999) 1731.
- 37 K. I. Ibragimov, A. C. Lushchik, C. B. Lushchik, A. Baimakhanov, and E. A. Vasil: *Sov. Phys. Solid State* **34** (1992) 3421.
- 38 J. K. Radhakrishnan and S. Selvasekarapandian: *J. Lumin.* **63** (1995) 137.
- 39 J. K. Radhakrishnan and S. Selvasekarapandian: *Phys. Status Solidi* **141** (1994) 457.